Electron-impact ionization in the iron isonuclear sequence

M. S. Pindzola

Department of Physics, Auburn University, Auburn, Alabama 36849

D. C. Griffin

Department of Physics, Rollins College, Winter Park, Florida 32789

C. Bottcher

Physics Division, Oak Ridge National Laboratory, Oak Ridge, Tennessee 37831

(Received 14 May 1986)

Excitation-autoionization contributions to the electron-impact ionization of Fe^{5+}, Fe^{6+}, Fe^{9+}, Fe^{11+}, and Fe^{13+} are calculated in the distorted-wave approximation. Calculations for Fe^{5+} which include only excitations from the $3p^6 3d^3$ ground configuration agree well with the experimental crossed beams measurements of Gregory et al. [preceding paper, Phys. Rev. A **34**, 3657 (1986)]. For Fe^{6+} the agreement between theory and experiment is also good. Calculations for Fe^{9+} are in reasonable agreement with experiment when only excitations from extremely metastable states of the $3p^4 3d$ excited configuration are included. Theoretical predictions for Fe^{11+} and Fe^{13+} are based on ground-configuration excitations and detailed branching-ratio calculations. Excitation-autoionization contributions in Fe^{13+} are found to enhance the total ionization cross section by a factor of 2 near threshold.

The theoretical study of electron-impact ionization processes in atomic ions has important applications in high-temperature plasma research. Of particular importance are studies along transition-metal isonuclear sequences which are directly applicable to numerical simulation of plasma cooling, transport, and confinement in experimental fusion devices.[1-3] However, isonuclear sequences present theoretical complications in that the atomic-structure changes along the series as various closed subshells open up. Thus no simple scaling laws of sufficient accuracy exist. Only a combination of experimental measurements and detailed theoretical scattering calculations can provide ionization cross sections to a 20% or better accuracy along an isonuclear series.

In the last decade experiment and theory have shown[4] that indirect resonance processes may make substantial contributions to the electron-impact ionization of transition-metal ions in low stages of ionization. Contributions to the electron-impact single-ionization cross section can be made by the following two processes:

$$e^- + A^{n+} \rightarrow A^{(n+1)+} + e^- + e^- , \tag{1}$$

and

$$e^- + A^{n+} \rightarrow (A^{n+})^* + e^-$$
$$\searrow A^{(n+1)+} + e^- , \tag{2}$$
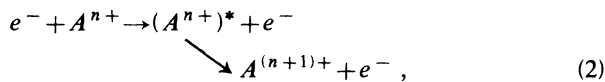
where A represents an arbitrary ion with charge n. The first process is direct ionization while the second is excitation autoionization. Although a complete quantum-mechanical description of electron ionization would include the wave-particle interference between these processes, for the purpose of obtaining a total cross section or rate they can generally be assumed to be independent of one another. A third process of resonant-recombination double autoionization is not considered in this work.[4]

The direct-ionization and excitation-autoionization processes may be calculated using the average-configuration distorted-wave method.[5] The most general direct-ionization transition between configurations is of the form

$$(n_1 l_1)^{q_1+1} k_i l_i \rightarrow (n_1 l_1)^{q_1} k_e l_e k_f l_f , \tag{3}$$

where n is the principal quantum number, l is the angular momentum quantum number, q is the occupation number, and k is the linear momentum wave number. The average-configuration direct-ionization cross section (in atomic units) is given by

$$\sigma_{\text{ion}} = \int_0^{E/2} \frac{32(q_1+1)}{k_i^3 k_e k_f} \sum_{l_i, l_e, l_f} (2l_i+1)(2l_e+1)(2l_f+1)$$

$$\times M(ef; 1i) , \tag{4}$$

where $E = (k_e^2 + k_f^2)/2$. The most general excitation transition between configurations is of the form

$$(n_1 l_1)^{q_1+1}(n_2 l_2)^{q_2-1} k_i l_i \rightarrow (n_1 l_1)^{q_1}(n_2 l_2)^{q_2} k_f l_f . \tag{5}$$

The average-configuration excitation cross section is given by

$$\sigma_{\text{exc}} = \frac{8\pi}{k_i^3 k_f}(q_1+1)(4l_2+3-q_2)$$

$$\times \sum_{l_i, l_f} (2l_i+1)(2l_f+1)M(2f; 1i) . \tag{6}$$

The continuum normalization in both Eqs. (4) and (6) is chosen as one times a sine function.

The scattering matrix element M in both Eqs. (4) and (6) is given by

$$M(14;23) = \sum_{\lambda} \begin{bmatrix} l_1 & \lambda & l_2 \\ 0 & 0 & 0 \end{bmatrix}^2 \begin{bmatrix} l_3 & \lambda & l_4 \\ 0 & 0 & 0 \end{bmatrix}^2 \frac{[R^\lambda(14;23)]^2}{(2\lambda+1)} + \sum_{\lambda'} \begin{bmatrix} l_1 & \lambda' & l_3 \\ 0 & 0 & 0 \end{bmatrix}^2 \begin{bmatrix} l_2 & \lambda' & l_4 \\ 0 & 0 & 0 \end{bmatrix}^2 \frac{[R^{\lambda'}(41;23)]^2}{(2\lambda'+1)}$$

$$- \sum_{\lambda} \sum_{\lambda'} (-1)^{\lambda+\lambda'} \begin{Bmatrix} l_1 & l_2 & \lambda \\ l_4 & l_3 & \lambda' \end{Bmatrix} \begin{bmatrix} l_1 & \lambda & l_2 \\ 0 & 0 & 0 \end{bmatrix} \begin{bmatrix} l_3 & \lambda & l_4 \\ 0 & 0 & 0 \end{bmatrix}$$

$$\times \begin{bmatrix} l_1 & \lambda' & l_3 \\ 0 & 0 & 0 \end{bmatrix} \begin{bmatrix} l_2 & \lambda' & l_4 \\ 0 & 0 & 0 \end{bmatrix} R^\lambda(14;23) R^{\lambda'}(41;23) , \tag{7}$$

where $R^\lambda(ij;rt)$ is the usual Slater radial integral and angular coefficients are summarized in terms of standard 3-j and 6-j symbols. Due to the presence of two outgoing continuum waves the phase of the interference term in Eq. (7) is arbitrary for the direct-ionization process. We employ the maximum interference approximation[6] which takes the negative of the absolute value of the third term on the right-hand side of Eq. (7). The bound-state energies and orbitals needed to evaluate Eqs. (4) and (6) are generated using the radial-wave-function code developed by Cowan.[7] The continuum orbitals are obtained by solving the radial Schrödinger equation in the distorted-wave approximation. For rapid evaluation of many continuum orbitals a local distorting potential constructed in a semiclassical exchange approximation[8] has proved useful.

The average-configuration distorted-wave method can be extended with little more effort to take into account the energy-level spread within each configuration. A simple procedure called the average-statistical model (ASM) is adopted. The average-configuration collision cross section for either the direct-ionization or excitation-autoionization process is statistically partitioned over all levels of the final ionized or excited configuration. The total cross section is then summed taking explicit account of the energy position of each level calculated using an atomic-structure program provided by Cowan.[7] If the atomic-structure calculations show that certain excited levels are bound, their contribution to the ionization cross section is of course ignored. Branching ratios for autoionization versus radiation are also calculated for each excited level and then multiplied by the statistically partitioned cross sections. A statistically weighted Boltzmann distribution over the levels of the initial configuration, based on an average ion temperature, may also be included in the average-statistical model.

Recently experimental crossed-beam measurements of ions in the Fe isonuclear sequence have been made.[9-11] Due to the formation characteristics of the ion sources, ion-beam currents generally become smaller for the higher ionization stages of a given element. More specifically the Oak Ridge National Laboratory (ORNL) ECR ion source and crossed-beams apparatus has been used to make measurements up to Fe^{9+}, although measurements up to Fe^{15+} should be possible. Thus comparison between experiment and theory is currently taking place in the lower ionization stages of Fe.

In previous work[5] on Fe^+ through Fe^{4+}, the $3p \rightarrow 3d$ dipole transition was found to dominate all other excitation-autoionization contributions. In Fe^{5+}, however, all the levels of the $3p^5 3d^4$ excited configuration are bound. In Table I the Fe^{5+} excitation energies and cross sections are listed. For excitation from the $3p^6 3d^3$ ground configuration, the $3p \rightarrow 4p$ monopole transition now dominates. In Fig. 1 an energy-level diagram shows the position of certain excited configurations of Fe^{5+} and Fe^{6+}. The $3p^5 3d^3 4p$ excited configuration of Fe^{5+} straddles the ionization threshold. Our atomic-structure calculations indicate that 419 of the 613 possible levels are autoionizing with an overall energy spread within the configuration of 37.3 eV. The next largest contribution is the $3s \rightarrow 3d$ quadrupole transition, where 58 of the 63 possible levels of the $3s 3p^6 3d^4$ configuration are autoionizing. In Fig. 2 the crossed-beams measurements of Gregory et al.[11] for Fe^{5+} are compared with an ASM calculation which includes all ten excitations from the ground configuration that are listed in Table I and an estimate for excitations to higher nl configurations. A combination of explicit calculation and n^3 rule extrapolation was used to approximate the high-nl excitation-autoionization contri-
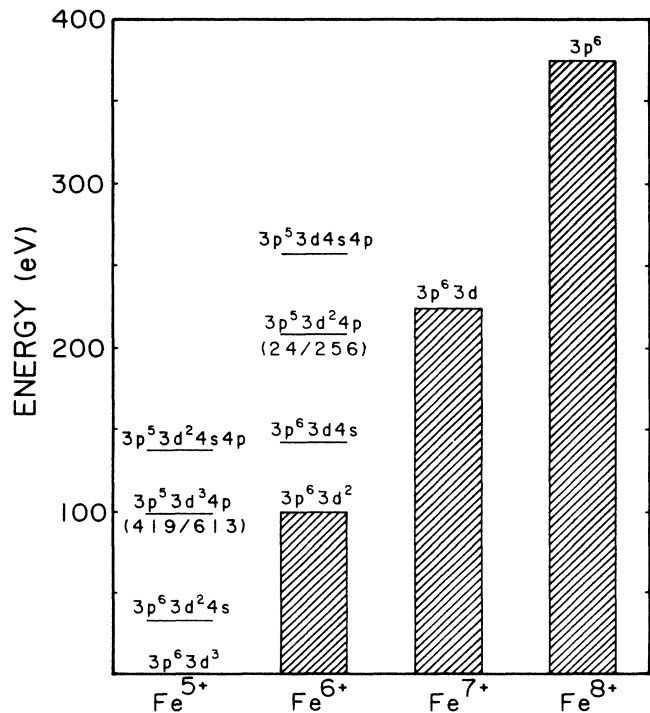

FIG. 1. Energy-level diagram showing various configurations of Fe^{5+} and Fe^{6+}. The ratio of autoionizing levels to the total number of levels is given below configurations which lie near the ionization threshold.

TABLE I. Fe^{5+} energies and cross sections.

Ion	Initial configuration	Excitation transition	Average excitation energy (eV)	Autoionizing to total levels ratio	Energy spread (eV)	Threshold cross section (10^{-18} cm^2)	Twice threshold cross section (10^{-18} cm^2)
Fe^{5+}	$3p^6 3d^3$	$3p \rightarrow 4s$	88.8	57/213	36.6	0.669	0.610
		$3p \rightarrow 4p$	98.5	419/613	37.3	4.848	2.789
		$3p \rightarrow 4d$	112.9	943/943	38.6	1.132	0.338
		$3p \rightarrow 4f$	123.3	1180/1180	36.7	0.759	0.453
		$3p \rightarrow 5p$	124.1	613/613	36.6	1.013	0.562
		$3p \rightarrow 5d$	130.1	943/943	36.7	0.370	0.101
		$3p \rightarrow 5f$	134.7	1180/1180	36.4	0.416	0.246
		$3s \rightarrow 3d$	99.4	58/63	24.5	2.636	1.675
		$3s \rightarrow 4s$	131.1	74/74	20.4	0.769	0.512
		$3s \rightarrow 5s$	162.3	74/74	19.8	0.145	0.095
	$3p^6 3d^2 4s$	$3p \rightarrow 3d$	57.5	57/213	36.6	73.755	49.511
		$3p \rightarrow 4s$	95.6	45/45	30.0	0.279	0.260
		$3p \rightarrow 4p$	104.4	494/494	37.8	4.639	2.623
		$3p \rightarrow 4d$	120.2	750/750	35.6	1.000	0.297
		$3p \rightarrow 4f$	131.5	924/924	32.4	0.821	0.476
		$3p \rightarrow 5p$	132.4	494/494	31.8	0.872	0.474
		$3p \rightarrow 5d$	138.6	750/750	32.3	0.308	0.087
		$3p \rightarrow 5f$	143.5	924/924	31.6	0.421	0.242
		$3s \rightarrow 3d$	99.8	74/74	20.4	3.096	1.864
		$3s \rightarrow 4s$	138.9	16/16	12.9	0.361	0.237

butions. The direct-ionization contribution includes $3s$, $3p$, and $3d$ subshell ionization from the ground configuration as calculated previously in the average-configuration distorted-wave approximation by Younger.[12] The agreement between theory and experiment is reasonably good. Near threshold the excitation-autoionization contribution enhances the direct ionization by more than a factor of 2. The smooth appearance of the theoretical curve results from the statistical partition of the total excitation collision cross section over more than 5000 levels.
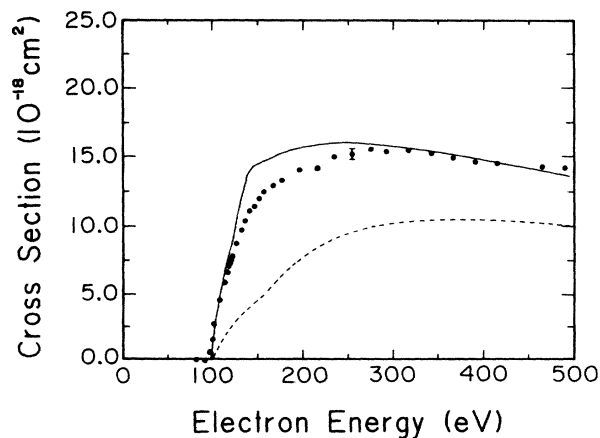
The ASM calculations on Fe^{5+} were repeated for

FIG. 2. Electron-impact ionization of Fe^{5+}. Solid curve, total cross section from the $3p^6 3d^3$ ground configuration in the average-statistical model; dashed curve, direct cross section only; solid circles, experimental measurements (Ref. 11).

electron-impact ionization from the $3p^6 3d^2 4s$ excited configuration. As shown in Fig. 1 the $3p^6 3d^2 4s$ configuration lies approximately 32 eV above the ground configuration. The 16 levels of $3p^6 3d^2 4s$ decay primarily by radiative quadrupole emission with lifetimes varying from 7.1 to 12.5 μsec as found from single-configuration atomic-structure calculations. The ratio of metastable excited states (μsec lifetimes or longer) in the excited $3p^6 3d^2 4s$ configuration to all states in the ground and excited configurations is 0.27. As shown in Table I, for excitation from the $3p^6 3d^2 4s$ excited configuration, the $3p \rightarrow 3d$ dipole transition dominates even though only 57 of the 213 possible levels of the $3p^5 3d^3 4s$ configuration are autoionizing. In Fig. 1 the $3p^5 3d^2 4s 4p$ configuration, resulting from a $3p \rightarrow 4p$ monopole transition, is seen to be well above the ionization limit. In Fig. 3 the crossed-beams measurements of Gregory et al.[11] for Fe^{5+} are compared with an ASM calculation which includes all ten excitations from the excited configuration that are listed in Table I. The direct-ionization contribution includes $3p$, $3d$, and $4s$ subshell ionization from the excited configuration. The agreement between theory and experiment is quite poor. The theoretical onset of ionization is off by at least 30 eV and the cross section near threshold is a factor of 2 high. It appears from comparing Figs. 2 and 3 that a substantial fraction of metastables in the $3p^6 3d^2 4s$ excited configuration have decayed before the measurements are made, even though the predicted lifetimes are in the μsec range.

In Table II the Fe^{6+} excitation energies and cross sections are listed. For excitation from the $3p^6 3d^2$ ground configuration, the $3p \rightarrow 4p$ monopole transition is cut down due to the fact that only 24 of the 256 levels of the
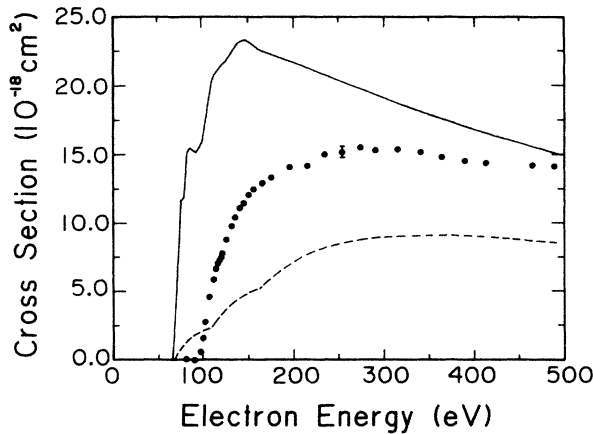
FIG. 3. Electron-impact ionization of Fe^{5+}. Solid curve, total cross section from the $3p^63d^24s$ excited configuration in the average-statistical model; dashed curve, direct cross section only; solid circles, experimental measurements (Ref. 11).
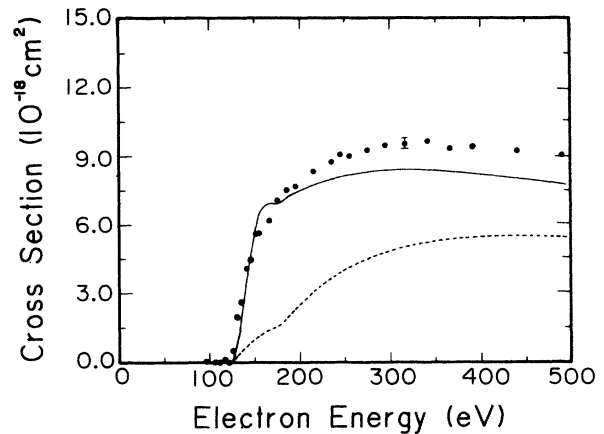

FIG. 4. Electron-impact ionization of Fe^{6+}. Solid curve, total cross section from the $3p^63d^2$ ground configuration in the average-statistical model; dashed curve, direct cross section only; solid circles, experimental measurements (Ref. 11).

$3p^53d^24p$ configuration are autoionizing. Actually the $3p\rightarrow4f$ quadrupole transition makes the largest excitation-autoionization contribution. In Fig. 4 the crossed-beams measurements of Gregory et al.[11] for Fe^{6+} are compared with an ASM calculation which includes all eight excitations from the ground configuration that are listed in Table II and an estimate for excitation to higher nl configurations. The direct-ionization contribution includes $3s$, $3p$, and $3d$ subshell ionization from the ground configuration as calculated previously by Younger.[12] The agreement between theory and experiment is reasonably good. The ASM calculations on Fe^{6+} were repeated for electron ionization from the $3p^63d4s$ excited configuration. As shown in Fig. 1 the $3p^63d4s$ configuration lies

approximately 43 eV above the ground configuration. The four levels of $3p^63d4s$ decay primarily by radiative quadrupole emission with calculated lifetimes varying from 2.0 to 3.4 μsec. The ratio of metastable excited states (μsec lifetimes or longer) in the excited $3p^63d4s$ configuration to all states in the ground and excited configurations is 0.31. As shown in Table II the $3p\rightarrow4p$ monopole transition in the excited configurations provides the largest contribution to the cross section. All 130 levels of the $3p^53d4s4p$ configuration are autoionizing. In Fig. 5 the crossed-beams measurements of Gregory et al.[11] for Fe^{6+} are compared with an ASM calculation which includes all nine excitations from the excited configuration that are listed in Table II. The direct-

TABLE II. Fe^{6+} energies and cross sections.

| Ion	Initial configuration	Excitation transition	Average excitation energy (eV)	Autoionizing to total levels ratio	Energy spread (eV)	Threshold cross section (10^{-18} cm^2)	Twice threshold cross section (10^{-18} cm^2)
Fe^{6+}	$3p^63d^2$	$3p\rightarrow4p$	108.8	24/256	32.1	4.645	2.557
		$3p\rightarrow4d$	124.8	204/386	34.1	0.927	0.305
		$3p\rightarrow4f$	136.6	472/472	31.7	1.104	0.647
		$3p\rightarrow5p$	140.1	256/256	30.8	0.927	0.492
		$3p\rightarrow5d$	147.0	386/386	31.7	0.298	0.097
		$3p\rightarrow5f$	152.2	472/472	31.1	0.534	0.306
		$3s\rightarrow4s$	141.2	32/32	15.6	0.777	0.484
		$3s\rightarrow5s$	178.6	32/32	13.9	0.140	0.087
	$3p^63d4s$	$3p\rightarrow4s$	105.3	12/12	25.9	0.232	0.229
		$3p\rightarrow4p$	114.9	130/130	33.8	4.398	2.386
		$3p\rightarrow4d$	132.2	192/192	30.2	0.825	0.285
		$3p\rightarrow4f$	144.9	226/226	28.3	1.162	0.669
		$3p\rightarrow5p$	148.9	130/130	27.4	0.804	0.419
		$3p\rightarrow5d$	155.9	192/192	27.2	0.253	0.089
		$3p\rightarrow5f$	161.4	226/226	26.9	0.519	0.292
		$3s\rightarrow3d$	99.7	32/32	15.6	3.667	2.064
		$3s\rightarrow4s$	149.4	4/4	6.0	0.361	0.223
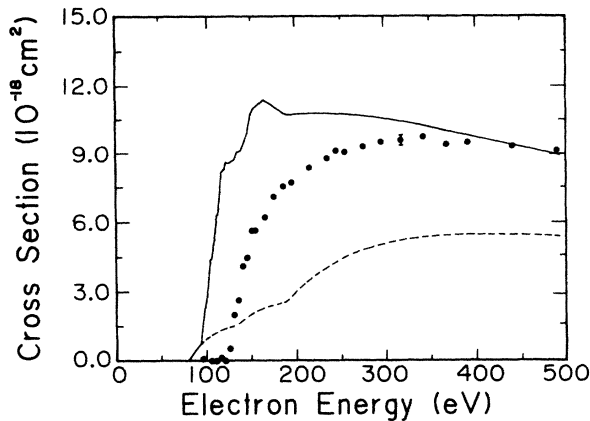
FIG. 5. Electron-impact ionization of Fe^{6+}. Solid curve, total cross section from the $3p^63d4s$ excited configuration in the average-statistical model; dashed curve, direct cross section only; solid circles, experimental measurements (Ref. 11).

ionization contributions include $3s$, $3p$, $3d$, and $4s$ subshell ionization from the excited configuration. The agreement between theory and experiment is quite poor. The theoretical onset of ionization is off by at least 40 eV. It appears from comparing Figs. 4 and 5 that a substantial number of metastables in the $3p^63d4s$ excited configuration have decayed before the measurements are made.

We proceeded to investigate the possibility that the source of the remaining discrepancy between experiment and the ASM ground-configuration calculations for Fe^{6+} lies in a nonstatistical distribution of the $3p\rightarrow4p$ collision cross section. It may happen that the 24 out of 256 levels that are autoionizing may contain most of the collision strength, thus a purely statistical distribution would underestimate the total cross section. A previous study[13] on Ti^{3+} based on a level-to-level intermediate-coupled distorted-wave calculation showed that the large $3p\rightarrow3d$ dipole transition cross section is indeed concentrated in the 6 out of 45 levels that are autoionizing.

A level-to-level intermediate-coupled distorted-wave calculation was carried out as described in earlier papers.[5,13] It may be divided into three parts. A general purpose computer code based on Racah algebra and Cowan's classification scheme[7] is used to calculate angular coefficients for the term-to-term transition matrix, $T(\beta_i L_i S_i J_i l_i \mathscr{L}\mathscr{S} \rightarrow \beta_f L_f S_f J_f l_f \mathscr{L}\mathscr{S})$, where L_i and S_i are the orbital and spin angular momenta of the target ion and $\mathscr{L}$ and $\mathscr{S}$ are the corresponding angular momenta for the electron-ion system. A second code uses bound orbitals generated by Cowan's radial wave-function code and continuum orbitals generated by a distorted-wave solution of the radial Schrödinger equation to calculate radial transition matrix elements. The final computer code uses standard recoupling procedures[7] to transform the T matrix from $\mathscr{L}\mathscr{S}$ coupling to Jj coupling. The energy eigenvalues and eigenvectors of each level calculated using an atomic-structure program provided by Cowan[7] are then used to construct the level-to-level transition matrix, $T(\alpha_i J_i l_i j_i \mathscr{f} \rightarrow \alpha_f J_f l_f j_f \mathscr{f})$. The level-to-level excitation cross section is then given by

$$\sigma_{exc} = \frac{16\pi}{k_i^3 k_f} \frac{1}{2(2J_i+1)}$$

$$\times \sum_{j_i,j_f} \sum_{l_i,l_f} \sum_{\mathscr{f}} (2\mathscr{f}+1)$$

$$\times \mid T(\alpha_i J_i l_i j_i \mathscr{f} \rightarrow \alpha_f J_f l_f j_f \mathscr{f}) \mid^2 .$$

Radiative branching ratios for each excited level are multiplied by each T matrix squared.

In Fig. 6 an average-configuration calculation for the $3p\rightarrow4p$ transition in Fe^{6+}, statistically distributed over the 256 levels of the $3p^53d^24p$ configuration, is compared with a level-to-level intermediate-coupled calculation. The distribution of collision cross section from the level-to-level calculation is seen to be fairly statistical. More importantly the 24 highest levels, those above the ionization limit of 125 eV, do not receive more than their statistical share of the total cross section. A level-to-level calculation for Fe^{6+} is thus almost identical to the ASM results shown in Fig. 4. It is interesting to note that for a many-level configuration, like $3p^53d^24p$, each energy point in a level-to-level calculation takes 30 min on a large vector processing machine while each energy point in an average-configuration calculation takes 4 sec. One may have to look to configuration interaction in the target states or continuum coupling of the bound and autoionizing levels to explain the remaining discrepancy.

In Table III the Fe^{9+} excitation energies and cross sections are listed. For excitation from the $3s^23p^5$ ground configuration, the $2p\rightarrow3d$ dipole transition is the largest contribution. Excitations from the $3s$ subshell are all to bound levels. In Fig. 7 an energy-level diagram places the $2p^53s^23p^53d$ configuration about 485 eV above the ionization limit. In Fig. 8 the crossed-beams measurements of Gregory et al.[11] for Fe^{9+} are compared with an ASM cal-
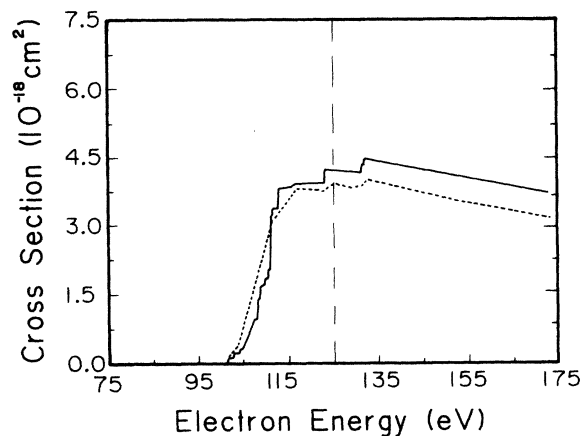

FIG. 6. Electron-impact excitation of Fe^{6+} from the $3p^63d^2$ ground configuration to all levels of the $3p^53d^24p$ excited configuration. Solid curve, level-to-level excitation cross section; dashed curve, average-configuration excitation cross section distributed statistically over all levels. Note that only those 24 out of 256 levels in the $3p^53d^24p$ configuration above the ionization limit at 125 eV are autoionizing.

TABLE III. Fe^{9+}, Fe^{11+}, and Fe^{13+} energies and cross sections.

Ion	Initial configuration	Excitation transition	Average excitation energy (eV)	Autoionizing to total levels ratio	Energy spread (eV)	Threshold cross section $(10^{-18}$ cm$^2)$	Twice threshold cross section $(10^{-18}$ cm$^2)$
Fe^{9+}	$3s^23p^5$	$2p\to3d$	746.9	65/65	44.3	0.187	0.119
	$3s^23p^43d$	$3s\to4d$	201.0	258/452	50.9	0.138	0.068
		$3s\to5s$	226.4	107/107	48.6	0.115	0.066
		$3s\to5p$	232.1	303/303	48.8	0.026	0.017
		$2p\to3p$	691.2	65/65	44.3	0.038	0.018
		$2p\to3d$	748.0	604/604	72.9	0.167	0.106
Fe^{11+}	$3s^23p^3$	$2p\to3p$	709.3	21/21	28.7	0.057	0.027
		$2p\to3d$	763.8	203/203	54.1	0.201	0.130
		$2p\to4p$	882.4	143/143	39.8	0.019	0.008
		$2p\to4d$	901.9	203/203	38.9	0.042	0.025
		$2s\to3d$	899.3	72/72	37.0	0.025	0.015
Fe^{13+}	$3s^23p$	$2p\to3p$	728.7	21/21	30.6	0.094	0.044
		$2p\to3d$	782.2	65/65	41.5	0.213	0.140
		$2p\to4p$	926.6	48/48	34.3	0.021	0.009
		$2p\to4d$	945.4	65/65	32.5	0.046	0.027
		$2s\to3d$	916.9	23/23	20.2	0.026	0.016

culation which includes the $2p\to3d$ ground-configuration excitation. The direct-ionization contribution includes $3s$ and $3p$ subshell ionization from the $3s^23p^5$ configuration as calculated by Younger.[12] The theory falls below experiment and does not predict the proper threshold energy. The ASM calculations on Fe^{9+} were repeated for electron
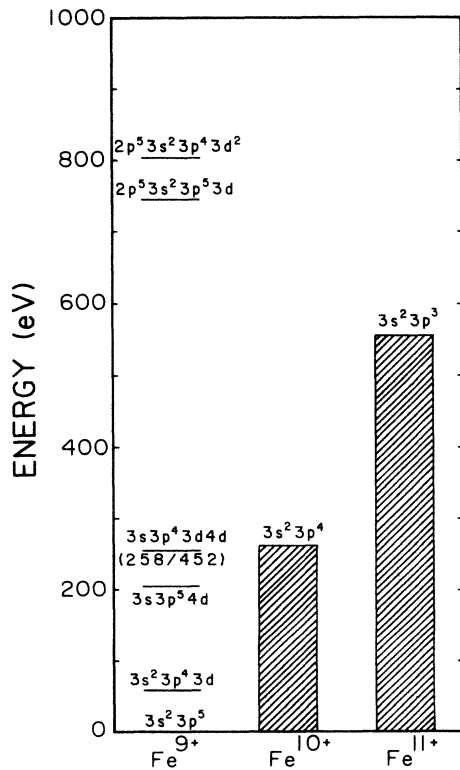
FIG. 7. Energy-level diagram showing various configurations of Fe^{9+}. The ratio of autoionizing levels to the total number of levels is given below configurations which lie near the ionization threshold.

ionization from the $3s^23p^43d$ excited configuration. As shown in Fig. 7 the $3s^23p^43d$ configuration lies approximately 48 eV above the ground configuration. Of the 150 states in the $3s^23p^43d$ configuration, 60 are forbidden to decay by J selection rules while the remaining 90 have calculated lifetimes ranging from 0.2 μsec to 3.7 psec. The ratio of extremely metastable excited states (msec lifetimes or longer) in the excited $3s^23p^43d$ configuration to all states of the ground and excited configurations is 0.38. As shown in Table III the $2p\to3d$ dipole transition in the excited configuration provides the largest contribution to the cross section. The now available $3s\to4d$ quadrupole transition is cut down due to the fact that only 258 of the 452 levels of $3s3p^43d4d$ configuration are autoionizing. In Fig. 9 the crossed-beams measurements of Gregory et al.[11] for Fe^{9+} are compared with an ASM calculation
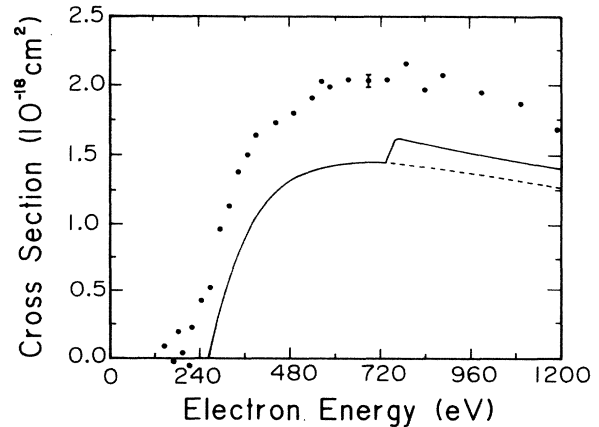
FIG. 8. Electron-impact ionization of Fe^{9+}. Solid curve, total cross section from the $3s^23p^5$ ground configuration in the average-statistical model; dashed curve, direct cross section only; solid circles, experimental measurements (Ref. 11).
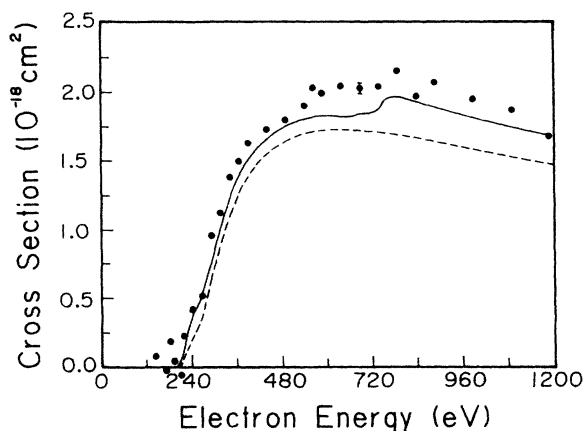
FIG. 9. Electron-impact ionization of Fe^{9+}. Solid curve, total cross section from the $3s^23p^43d$ excited configuration in the average-statistical model; dashed curve, direct cross section only; solid circles, experimental measurements (Ref. 11).

which includes all five excitations from the excited configuration that are listed in Table III. The direct-ionization contributions include $3s$, $3p$, and $3d$ subshell ionization from the excited configuration. The agreement between theory and experiment has improved substantially. It seems that the experiment on Fe^{9+} is predominantly measuring electron ionization from the extremely meta-

stable levels of the excited configuration.

Although no experimental measurements as yet exist, average-statistical model calculations were made for the electron-impact ionization of Fe^{11+} and Fe^{13+}. In Table III the Fe^{11+} and Fe^{13+} excitation energies and cross sections are listed. The $2p \rightarrow 3d$ dipole transition makes the largest contribution in both atomic ions. As one moves along the isonuclear sequence to the higher ionization stages radiative branching generally becomes more important. In complex configurations, however, care must be taken to include all possible autoionization and radiative decay channels. In Table IV the possible decay channels are listed for a couple of doubly excited configurations in both Fe^{11+} and Fe^{13+}. The branching ratios for most of the autoionizing levels in both Fe^{11+} and Fe^{13+} are close to 1.0, principally due to the fact that so many autoionizing decay channels are present. In Fig. 10 the results are shown of an ASM calculation for Fe^{11+}, while Fig. 11 presents the Fe^{13+} results. In both cases all five excitations from the ground configuration that are listed in Table III are included. The direct-ionization contributions include $3s$ and $3p$ subshell ionization as calculated by Younger.[12] Even for the highly ionized Fe^{13+} case, the contributions from excitation autoionization are still quite important. ASM calculations on Fe^{11+} and Fe^{13+} were not made for electron ionization from excited configurations. In Fe^{11+}, the ratio of extremely metastable excited states (msec lifetimes or longer) in the excited $3s^23p^23d$

TABLE IV: Fe^{11+} and Fe^{13+} branching-ratio channels.

| Ion	Excitation transition	Doubly excited configuration	Autoionization decay channel	Radiative decay channel
Fe^{11+}	$2p \rightarrow 3p$	$2p^53s^23p^4$	$2p^63s^23p^2kp$ $2p^63s^23p^2kf$ $2p^63s3p^3ks$ $2p^63s3p^3kd$ $2p^63p^4kp$	$2p^63s3p^4$
	$2p \rightarrow 3d$	$2p^53s^23p^33d$	$2p^63s^23p^2ks$ $2p^63s^23p^2kd$ $2p^63s^23p^2kg$ $2p^63s^23p3dkp$ $2p^63s^23p3dkf$ $2p^63s3p^3kp$ $2p^63s3p^3kf$ $2p^63s3p^23dks$ $2p^63s3p^23dkd$ $2p^63p^33dkp$	$2p^63s^23p^3$ $2p^63s3p^33d$
Fe^{13+}	$2p \rightarrow 3p$	$2p^53s^23p^2$	$2p^63s^2kp$ $2p^63s^2kf$ $2p^63s3pks$ $2p^63s3pkd$ $2p^63p^2kp$	$2p^63s3p^2$
	$2p \rightarrow 3d$	$2p^53s^23p3d$	$2p^63s^2ks$ $2p^63s^2kd$ $2p^63s^2kg$ $2p^63s3pkp$ $2p^63s3pkf$ $2p^63s3dks$ $2p^63s3dkd$ $2p^63p3dkp$	$2p^63s^23p$ $2p^63s3p3d$
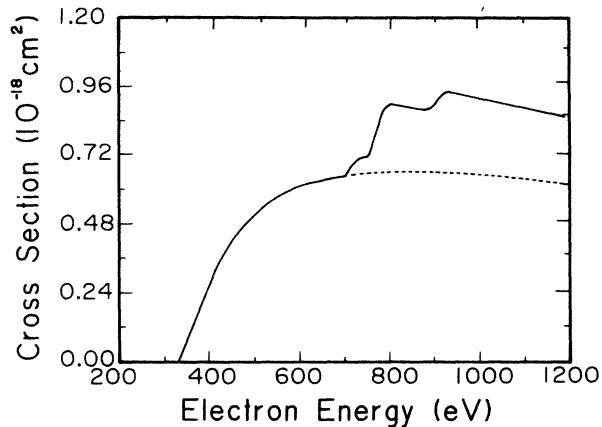
FIG. 10. Electron-impact ionization of Fe^{11+}. Solid curve, total cross section from the $3s^2 3p^3$ ground configuration in the average-statistical model; dashed curve, direct cross section only.

FIG. 11. Electron-impact ionization of Fe^{13+}. Solid curve, total cross section from the $3s^2 3p$ ground configuration in the average-statistical model; dashed curve, direct cross section only.

configuration to all states of the ground and excited configurations is 0.07; while in Fe^{13+} there are no low-lying metastable states.

Although much work remains to be done to understand electron-impact ionization along the Fe isonuclear sequence, the comparison of experimental crossed-beams measurements and average-statistical model calculations brings certain features into focus. The rather smooth sequence of experimental points in Fe^{5+} and Fe^{6+} does not mark the absence of excitation-autoionization contributions, but results from the blending of excitations to thousands of autoionizing levels. For these ions detailed level to level distorted-wave calculations become tedious, while the study of more complicated configuration-interaction and continuum-coupling effects is very difficult. It appears that contributions from metastable states of excited configurations in both Fe^{5+} and Fe^{6+} are small in the experiment of Gregory et al.[11] In Fe^{9+} the situation is reversed, reasonable agreement between theory and experiment is found when only ionization from extremely metastable states (in the msec range) of the $3p^4 3d$ excited configuration is considered dominant. The fact that ioni-
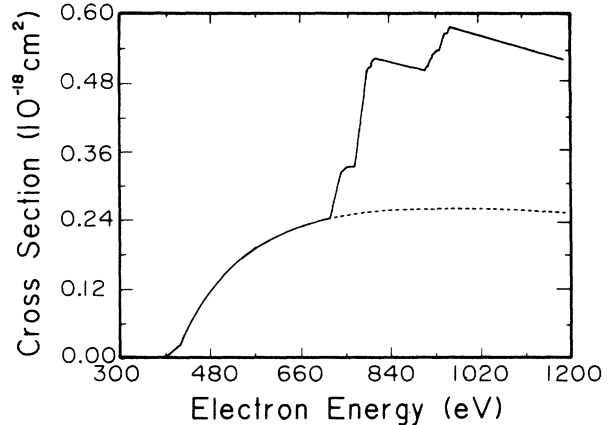
zation cross sections are sensitive to the lifetimes of metastable excited states makes the study of short-time scale modeling of an Fe-seeded plasma even more difficult. Finally significant excitation-autoionization contributions were found in the highest ions studied. Branching ratios close to 1.0 for the majority of autoionizing levels in Fe^{11+} and Fe^{13+} kept the excitation-autoionization contribution constant as the direct ionization fell in magnitude. The ASM calculations predict a total ionization cross section in Fe^{13+} approximately double that coming from previous direct-ionization calculations.

ACKNOWLEDGMENTS

[1]D. F. Duchs, D. E. Post, and P. H. Rutherford, Nucl. Fusion 17, 565 (1977).

[2]R. A. Hulse, Nucl. Technol. Fusion 3, 259 (1983).

[3]R. W. P. McWhirter and H. P. Summers, in Applied Atomic Collision Physics, edited by C. F. Barnett and M. F. A. Harrison (Academic, New York, 1984), Vol. 2, p. 51.

[4]D. H. Crandall, in Physics of Electron and Atomic Collisions; Invited Papers of the Twelfth International Conference on the Physics of Electronic and Atomic Collisions, edited by S. Datz (North-Holland, Amsterdam, 1982), p. 595.

[5]M. S. Pindzola, D. C. Griffin, C. Bottcher, D. C. Gregory, A. M. Howald, R. A. Phaneuf, D. H. Crandall, G. H. Dunn, D. W. Mueller, and T. J. Morgan, ORNL Report No. TM-9436, 1985 (unpublished).

[6]R. K. Peterkop, Zh. Eksp. Teor. Fiz. 41, 1938 (1961) [Sov. Phys.—JETP 14, 1377 (1962)].

[7]R. D. Cowan, The Theory of Atomic Structure and Spectra (California, Berkeley, 1981).

[8]M. E. Riley and D. G. Truhlar, J. Chem. Phys. 63, 2182 (1975).

[9]R. G. Montague, M. J. Diserens, and M. F. A. Harrison, J. Phys. B 17, 2085 (1984).

[10]D. W. Mueller, T. J. Morgan, G. H. Dunn, D. C. Gregory, and D. H. Crandall, Phys. Rev. A 31, 2905 (1985).

[11]D. C. Gregory, F. W. Meyer, A. Müller, and P. DeFrance, preceding paper, Phys. Rev. A 34, 3657 (1986).

[12]S. M. Younger, At. Data Fusion 7, 190 (1981).

[13]C. Bottcher, D. C. Griffin, and M. S. Pindzola, J. Phys. B 16, L65 (1983).